Mechanism and Machine Theory 45 (2010) 772–779

Contents lists available at ScienceDirect

Mechanism and Machine Theory

journal homepage: www.elsevier.com/locate/mechmt

The line-symmetric octahedral Bricard linkage and its structural closure

W.H. Chai, Y. Chen *

School of Mechanical and Aerospace Engineering, Nanyang Technological University, Singapore, 50 Nanyang Avenue, Singapore 639798, Singapore

ARTICLE INFO

Article history:
Received 18 August 2009
Received in revised form 16 December 2009
Accepted 16 December 2009
Available online 13 January 2010

Keywords:
Bricard linkage
Overconstrained mechanism
Mobile octahedral
Structural closure

ABSTRACT

This paper deals with one of six distinct types of Bricard 6*R* linkages, the line-symmetric octahedral case. By analysing the closure equations of the linkage, we have found that with the six zero-length links of the same twist and the six revolute joints of the same offset, a special line-symmetric octahedral Bricard linkage can be formed. Moreover, one or two structural closures always exist with the identical set of links and joints. This characteristic could be used for the reconfigurable structure design.

1. Introduction

Among six-bar overconstrained mechanisms with revolute joints, the most remarkable are 'Bricard linkages'. Bricard first described three different types of mobile octahedra in 1897 [1], namely the line-symmetric, plane-symmetric and double collapsible cases. And 30 years later, he found three additional types of mobile linkages, namely the line-symmetric, the plane-symmetric and the trihedral linkages [2]. A thorough analysis of all six Bricard linkages was done by Baker [3], who delineated them by appropriate sets of independent closure equations. Bennett [4] studied the geometry of the three types of deformable octahedra, and presented the kinematic properties of these mechanisms. Interestingly Baker [5] found that a special line-symmetric Bricard's octahedral case with all six twists equal to $\arccos(-1/3)$ is equivalent of flexible form of the carbon skeleton of the cyclohexane molecule, known as boat form, and the linkage's stationary configurations are precisely equivalent to the minimum energy conformations of the flexing cyclohexane molecule. Meanwhile, the cyclohexane molecule also has a stable state, known as chair form, which indicates the existing of a rigid closure of the corresponding Bricard's octahedral case. Baker [6] also mentioned another such example that line-symmetric Bricard's octahedral case with all six twists equal to $\pi/2$ has a structural form without line of symmetry. These two examples evoke the question, for the line-symmetric octahedral case of Bricard linkage, is there always a structural closure corresponding to the mobile octahedral when the six zero-length links have the same twist and six joints have the same offset? This paper is devoted to the solution.

The layout of the paper is as follows. Section 2 gives a brief introduction of six distinct types of Bricard linkages and defines the geometric parameter of the special line-symmetric octahedral case that we study in this paper. In Section 3, we analyse the loop closure equation of the linkage to generate the kinematic paths of the mobile octahedron and its corresponding structural closure. The conclusions and discussion in Section 4 end the paper.

* Corresponding author. Tel.: +65 6790 5941; fax: +65 6790 4062.
E-mail address: chenyan@ntu.edu.sg (Y. Chen).

0094-114X/$ - see front matter © 2009 Elsevier Ltd. All rights reserved.
doi:10.1016/j.mechmachtheory.2009.12.007

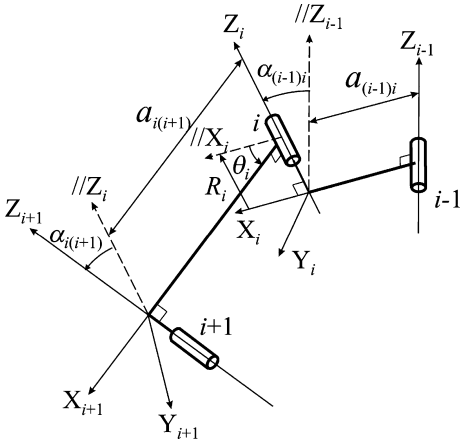

Fig. 1. Coordinate systems, parameters and variables for two adjacent links connected by revolute joints.

2. The Bricard linkages

For the links connected by revolute joint, coordinate system can be set up as shown in Fig. 1. Let us define the length of a link, $a_{i(i+1)}$, as the distance between the axes of two neighbouring revolute joints; the twist, $\alpha_{i(i+1)}$, as the skewed angle between the axes of two revolute joints at the ends of a link; the offset, R_i, as the distance between two links connected by the same revolute joint; the revolute variable, θ_i, as the angle between two axes of links connected by the same revolute joint.

The six distinct types of Bricard linkages can be summarised as follows [3,7]:

(a) *The general line-symmetric case*

$$\begin{aligned} &a_{12}=a_{45},\quad a_{23}=a_{56},\quad a_{34}=a_{61}\\ &\alpha_{12}=\alpha_{45},\quad \alpha_{23}=\alpha_{56},\quad \alpha_{34}=\alpha_{61},\\ &R_1=R_4,\quad R_2=R_5,\quad R_3=R_6. \end{aligned} \tag{1}$$

(b) *The general plane-symmetric case*

$$\begin{aligned} &a_{12}=a_{61},\quad a_{23}=a_{56},\quad a_{34}=a_{45}\\ &\alpha_{12}+\alpha_{61}=\pi,\quad \alpha_{23}+\alpha_{56}=\pi,\quad \alpha_{34}+\alpha_{45}=\pi,\\ &R_1=R_4=0,\quad R_2=R_6,\quad R_3=R_5. \end{aligned} \tag{2}$$

(c) *The trihedral case*

$$\begin{aligned} &a_{12}^2+a_{34}^2+,\quad a_{56}^2=a_{23}^2+,\quad a_{45}^2+a_{61}^2,\\ &\alpha_{12}=\alpha_{34},\quad \alpha_{56}=\frac{\pi}{2},\quad \alpha_{23}=\alpha_{45}=\alpha_{61}=\frac{3\pi}{2}\\ &R_i=0\quad (i=1,2,\ldots,6). \end{aligned} \tag{3}$$

(d) *The line-symmetric octahedral case*

$$\begin{aligned} &a_{12}=a_{23}=a_{34}=a_{45}=a_{56}=a_{61}=0,\\ &R_1+R_4=R_2+R_5=R_3+R_6=0. \end{aligned} \tag{4}$$

(e) *The plane-symmetric octahedral case*

$$\begin{aligned} &a_{12}=a_{23}=a_{34}=a_{45}=a_{56}=a_{61}=0,\\ &R_4=R_1,\quad R_2=R_1\frac{\sin\alpha_{34}}{\sin(\alpha_{12}+\alpha_{34})},\quad R_5=R_1\frac{\sin\alpha_{61}}{\sin(\alpha_{45}+\alpha_{61})},\\ &R_3=R_1\frac{\sin\alpha_{12}}{\sin(\alpha_{12}+\alpha_{34})},\quad R_6=-R_1\frac{\sin\alpha_{45}}{\sin(\alpha_{45}+\alpha_{61})} \end{aligned} \tag{5}$$

(f) *The doubly collapsible octahedral case*

$$\begin{aligned} &a_{12}=a_{23}=a_{34}=a_{45}=a_{56}=a_{61}=0,\\ &R_1R_3R_5+R_2R_4R_6=0. \end{aligned} \tag{6}$$

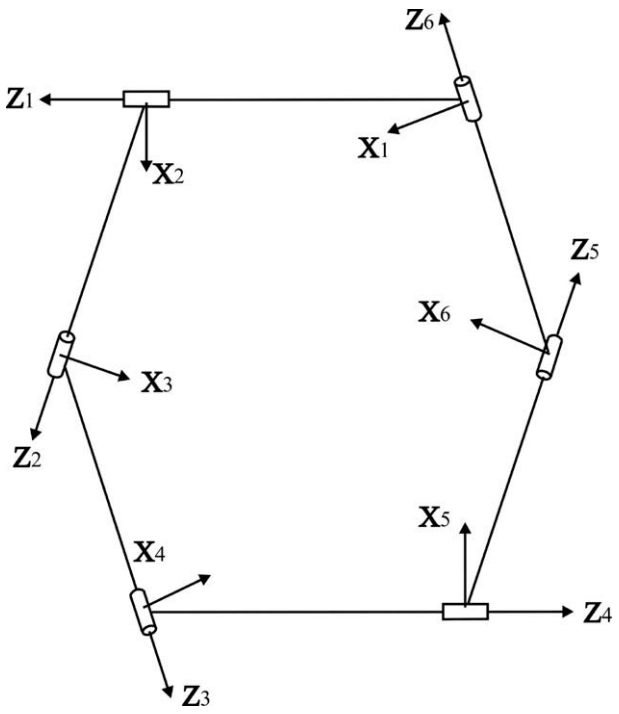

Fig. 2. Schematic diagram of line-symmetric octahedral Bricard linkage.

Here, we draw our attention to a special line-symmetric octahedral Bricard linkage with geometric parameters as follows.

$$\begin{aligned} &a_{12} = a_{23} = a_{34} = a_{45} = a_{56} = a_{61} = 0,\\ &\alpha_{12} = \alpha_{23} = \alpha_{34} = \alpha_{45} = \alpha_{56} = \alpha_{61} = \alpha,\\ &R_1 = R_2 = R_3 = R_4 = R_5 = R_6 = R. \end{aligned} \tag{7}$$

Schematic diagram of such linkage is shown in Fig. 2.

3. The loop closure equation

Denavit and Hartenberg [8] set forth a standard approach to the analysis of linkages. For a simple close-loop in a linkage, the product of all the transform matrices equals the unit matrix. So the *loop closure equation* becomes

$$\mathbf{T}_{n1}\cdots\mathbf{T}_{34}\mathbf{T}_{23}\mathbf{T}_{12} = \mathbf{I}, \tag{8}$$

where

$$\mathbf{T}_{i(i+1)} = \begin{bmatrix} C\theta_i & S\theta_i & 0 & -a_{i(i+1)} \\ -C\alpha_{i(i+1)}S\theta_i & C\alpha_{i(i+1)}C\theta_i & S\alpha_{i(i+1)} & -R_iS\alpha_{i(i+1)} \\ S\alpha_{i(i+1)}S\theta_i & -S\alpha_{i(i+1)}C\theta_i & C\alpha_{i(i+1)} & -R_iC\alpha_{i(i+1)} \\ 0 & 0 & 0 & 1 \end{bmatrix}, \tag{9}$$

where '*C*' is for 'cos' and '*S*' is for 'sin', and when $i+1>n$, $i+1$ is replaced by 1.

Note that the transfer matrix between the system of link $i(i+1)$ and the system of link $(i-1)i$ is the inverse of $\mathbf{T}_{i(i+1)}$. That is

$$\mathbf{T}_{(i+1)i} = \mathbf{T}_{i(i+1)}^{-1} = \begin{bmatrix} C\theta_i & -C\alpha_{i(i+1)}S\theta_i & S\alpha_{i(i+1)}S\theta_i & a_{i(i+1)}C\theta_i \\ S\theta_i & C\alpha_{i(i+1)}C\theta_i & -S\alpha_{i(i+1)}C\theta_i & a_{i(i+1)}S\theta_i \\ 0 & S\alpha_{i(i+1)} & C\alpha_{i(i+1)} & R_i \\ 0 & 0 & 0 & 1 \end{bmatrix}. \tag{10}$$

For the special line-symmetric octahedral Bricard linkage with geometric parameters listed in (7), there are six revolute variables, $\theta_i (i = 1, 2, \ldots, 6)$. Following (8)–(10), the loop closure equation can be derived as

$$\mathbf{T}_{21}\mathbf{T}_{32}\mathbf{T}_{43} = \mathbf{T}_{61}\mathbf{T}_{56}\mathbf{T}_{45}. \tag{11}$$

The left and right sides of (11) are both 4×4 matrices in the form

$$\mathbf{T} = \begin{bmatrix} t_{11} & t_{12} & t_{13} & t_{14} \\ t_{21} & t_{22} & t_{23} & t_{24} \\ t_{31} & t_{32} & t_{33} & t_{34} \\ t_{41} & t_{42} & t_{43} & t_{44} \end{bmatrix}$$

so their 16 elements should be equal correspondingly. The 3×3 sub-matrix on the left-up corner is rotation transfer matrix, while the 3×1 sub-matrix on the right-up corner is the translation vector, and the fourth row is always $[0 \quad 0 \quad 0 \quad 1]$ due to (9) and (10). Substituting all geometric parameters in (7) into (11), 12 equations and 4 identities can be obtained. Three of them are the elements of translation vector,

$$S\alpha S\theta_1 + C\alpha S\alpha S\theta_1 + C\alpha S\alpha S\theta_1 C\theta_2 + S\alpha C\theta_1 S\theta_2 = -S\alpha S\theta_6 - C\alpha S\alpha S\theta_6 - S\alpha S\theta_5 C\theta_6 - C\alpha S\alpha C\theta_5 S\theta_6, \tag{12}$$

$$\begin{aligned} -S\alpha C\theta_1 - C\alpha S\alpha C\theta_1 - C\alpha S\alpha C\theta_1 C\theta_2 + S\alpha S\theta_1 S\theta_2 &= -S\alpha - C\alpha S\alpha - C\alpha S\alpha C\theta_6 - C^2\alpha S\alpha - C^2\alpha S\alpha C\theta_6 \\ &\quad - C^2\alpha S\alpha C\theta_5 C\theta_6 + S^3\alpha C\theta_5 + C\alpha S\alpha S\theta_5 S\theta_6, \end{aligned} \tag{13}$$

$$1 + C\alpha + C^2\alpha - S^2\alpha C\theta_2 = -C\alpha - C^2\alpha + S^2\alpha C\theta_6 - C^3\alpha + C\alpha S^2\alpha C\theta_6 + C\alpha S^2\alpha C\theta_5 + C\alpha S^2\alpha C\theta_5 C\theta_6 - S^2\alpha S\theta_5 S\theta_6, \tag{14}$$

which are for elements t_{14}, t_{24}, and t_{34}, respectively. And for the element t_{32}, we have

$$\begin{aligned} &C^2\alpha S\alpha + C^2\alpha S\alpha C\theta_3 + C^2\alpha S\alpha C\theta_2 C\theta_3 - S^3\alpha C\theta_2 - C\alpha S\alpha S\theta_2 S\theta_3 \\ &\quad = -C^2\alpha S\alpha C\theta_4 C\theta_5 C\theta_6 + S^3\alpha C\theta_4 C\theta_6 + C\alpha S\alpha S\theta_4 S\theta_5 C\theta_6 - C^2\alpha S\alpha C\theta_4 - C^2\alpha S\alpha C\theta_4 C\theta_5 + C\alpha S\alpha S\theta_4 S\theta_5 + S\alpha S\theta_4 C\theta_5 S\theta_6 \\ &\qquad + C\alpha S\alpha C\theta_4 S\theta_5 S\theta_6. \end{aligned} \tag{15}$$

Similarly, when the loop closure equation is written as

$$\mathbf{T}_{56}\mathbf{T}_{45}\mathbf{T}_{34} = \mathbf{T}_{16}\mathbf{T}_{21}\mathbf{T}_{32}$$

the elements of translation vector elements t_{14}, t_{24}, and t_{34} are

$$S\alpha S\theta_5 + C\alpha S\alpha S\theta_5 + S\alpha S\theta_4 C\theta_5 + C\alpha S\alpha C\theta_4 S\theta_5 = -S\alpha S\theta_6 - C\alpha S\alpha S\theta_6 - S\alpha C\theta_6 S\theta_1 - C\alpha S\alpha S\theta_6 C\theta_1, \tag{16}$$

$$\begin{aligned} &C\alpha S\alpha + C\alpha S\alpha C\theta_5 + C^2\alpha S\alpha + C^2\alpha S\alpha C\theta_5 + C^2\alpha S\alpha C\theta_4 C\theta_5 - S^3\alpha C\theta_4 - C\alpha S\alpha S\theta_4 S\theta_5 \\ &\quad = -S\alpha + S\alpha C\theta_6 + C\alpha S\alpha C\theta_6 + C\alpha S\alpha C\theta_6 C\theta_1 - S\alpha S\theta_6 S\theta_1, \end{aligned} \tag{17}$$

$$1 + C\alpha + C^2\alpha - S^2\alpha C\theta_1 = -C\alpha - C^2\alpha + S^2\alpha C\theta_5 - C^3\alpha + C\alpha S^2\alpha C\theta_5 + C\alpha S^2\alpha C\theta_4 + C\alpha S^2\alpha C\theta_4 C\theta_5 - S^2\alpha S\theta_4 S\theta_5. \tag{18}$$

When the loop closure equation is written as

$$\mathbf{T}_{45}\mathbf{T}_{34}\mathbf{T}_{23} = \mathbf{T}_{65}\mathbf{T}_{16}\mathbf{T}_{21}$$

the elements of translation vector elements t_{14}, t_{24}, and t_{34} are

$$S\alpha S\theta_4 + C\alpha S\alpha S\theta_4 + S\alpha S\theta_3 C\theta_4 + C\alpha S\alpha C\theta_3 S\theta_4 = -S\alpha S\theta_5 - C\alpha S\alpha S\theta_5 - S\alpha C\theta_5 S\theta_6 - C\alpha S\alpha S\theta_5 C\theta_6 \tag{19}$$

$$\begin{aligned} &C\alpha S\alpha + C\alpha S\alpha C\theta_4 + C^2\alpha S\alpha + C^2\alpha S\alpha C\theta_4 + C^2\alpha S\alpha C\theta_3 C\theta_4 - S^3\alpha C\theta_3 - C\alpha S\alpha S\theta_3 S\theta_4 \\ &\quad = -S\alpha + S\alpha C\theta_5 + C\alpha S\alpha C\theta_5 + C\alpha S\alpha C\theta_5 C\theta_6 - S\alpha S\theta_5 S\theta_6, \end{aligned} \tag{20}$$

$$1 + C\alpha + C^2\alpha - S^2\alpha C\theta_6 = -C\alpha - C^2\alpha + S^2\alpha C\theta_4 - C^3\alpha + C\alpha S^2\alpha C\theta_4 + C\alpha S^2\alpha C\theta_3 + C\alpha S^2\alpha C\theta_3 C\theta_4 - S^2\alpha S\theta_3 S\theta_4. \tag{21}$$

Then $\frac{[(16)^2+(17)^2+(18)^2]}{-2S\alpha} - (15)$ yields

$$S\alpha C\theta_1 = S\alpha C\theta_4.$$

When $\alpha \neq 0$ or π,

$$\theta_1 = \pm\theta_4. \tag{22a}$$

Following the similar derivation, we can also obtain that

$$\theta_2 = \pm\theta_5, \tag{22b}$$

and

$$\theta_3 = \pm\theta_6. \tag{22c}$$

In (22), there are eight combinations. Here we only discuss following two cases,

$$\theta_1 = \theta_4, \quad \theta_2 = \theta_5, \quad \text{and} \quad \theta_3 = \theta_6;$$
$$\theta_1 = -\theta_4, \quad \theta_2 = -\theta_5, \quad \text{and} \quad \theta_3 = -\theta_6,$$

as the rest six cases are covered by the solution of Case I for certain special positions.

Case I:

$$\theta_1 = \theta_4, \quad \theta_2 = \theta_5, \quad \text{and} \quad \theta_3 = \theta_6. \tag{23}$$

Considering the geometric condition of the linkage (7) and (23), the linkage moves with a line of symmetry. Substituting (23) into loop closure equation (18) gives

$$1 + 2C\alpha + 2C^2\alpha + C^3\alpha = S^2\alpha[(1 + C\alpha)(C\theta_1 + C\theta_2) + C\alpha C\theta_1 C\theta_2 - S\theta_1 S\theta_2]. \tag{24}$$

Similarly, (14) gives

$$1 + 2C\alpha + 2C^2\alpha + C^3\alpha = S^2\alpha[(1 + C\alpha)(C\theta_2 + C\theta_3) + C\alpha C\theta_2 C\theta_3 - S\theta_2 S\theta_3]. \tag{25}$$

The five equations in (23)–(25) in are a set of independent closure equations for the line-symmetric octahedral case of Bricard linkage with the geometric condition (7). Therefore the linkage has only one degree of mobility. Its kinematic paths are shown in Fig. 3 for different twist α.

From Fig. 3, a number of characteristics of the linkage can be found.

1. When $-\frac{\pi}{3} < \alpha < \frac{\pi}{3}$, there is no kinematic path, i.e., there is no such linkage and six links cannot form a closed loop;
2. when $\alpha = \pm\frac{\pi}{3}$, there is only one point on the kinematic path, $\theta_i = 0$ ($i = 1, 2, \ldots, 6$), i.e., the linkage forms a planar close-loop structure, which has infinitesimal mobility;
3. when $-\frac{2\pi}{3} < \alpha < -\frac{\pi}{3}$ and $\frac{\pi}{3} < \alpha < \frac{2\pi}{3}$, the kinematic path is a closed curve in one period, i.e., linkage moves continuously without physical blockage;
4. when $\alpha = \pm\frac{2\pi}{3}$, there is one configuration that six links form two-layer overlapped close-loop when $\theta_1 = 0$ or $\theta_1 = \pm\pi$. At this configuration, both the fifth and forth singular values of the Jacobian matrix are equal to zero, which indicate the decrease of the kinematic determinacy [9]. So it is a position with two degrees of bifurcation;
5. when $-\pi < \alpha < -\frac{2\pi}{3}$ and $\frac{2\pi}{3} < \alpha < \pi$, the kinematic path is four open curve in one period, i.e., linkage moves with physical blockage when one of six kinematic variable reach $\pm\pi$;

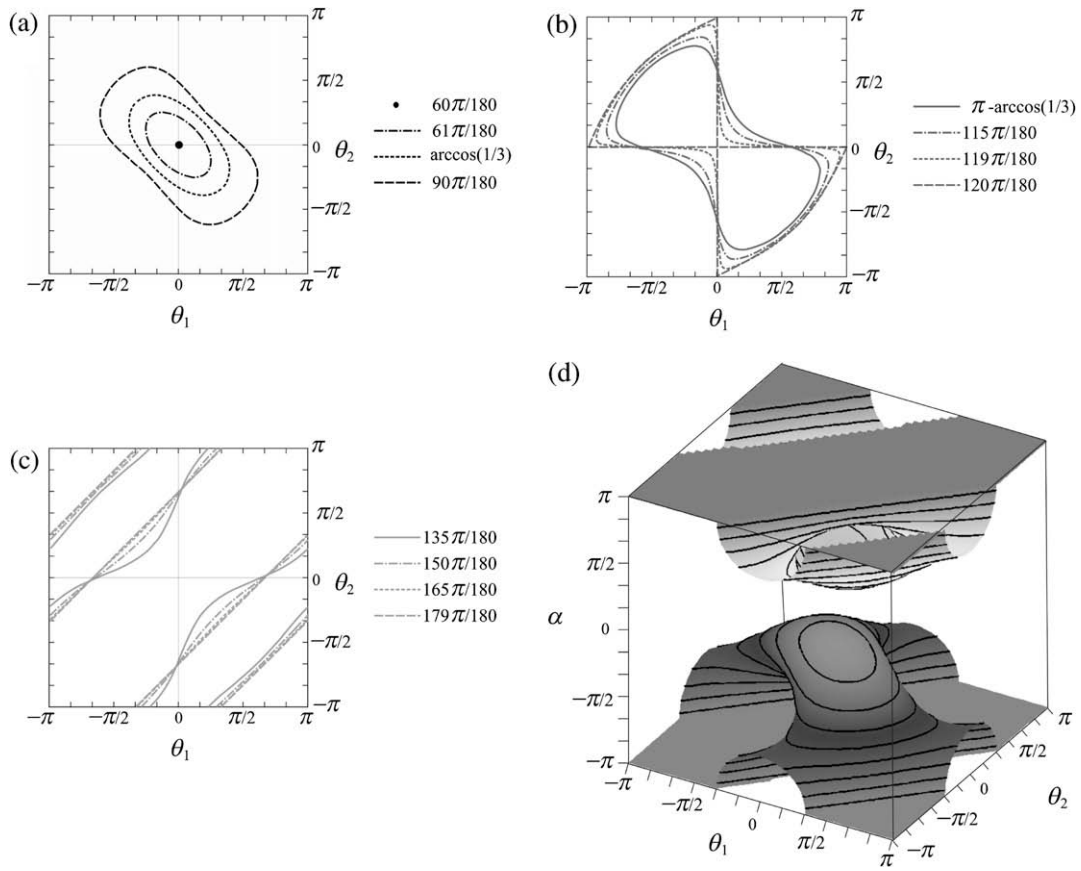

Fig. 3. The kinematic path of θ_2 vs. θ_1 for different twist α. (a)–(c) in 2D; (d) in 3D.

6. when $\alpha = \pm\pi$, the linkage will have six degrees of mobility because all six revolute joints have the same axis; and
7. linkages with twist α and $-\alpha$ have the same kinematic path, i.e., they are the same linkage with different setups of geometric parameters.

The motion sequence of model with $\alpha = \arccos(1/3)$, and $\alpha = \frac{3\pi}{4}$ is shown in Figs. 4 and 5, respectively.

Case II:

$$\theta_1 = -\theta_4, \quad \theta_2 = -\theta_5, \quad \text{and} \quad \theta_3 = -\theta_6. \tag{26}$$

Substituting (26) into (12),(13),(14) and (16),(17),(18),(19),(20),(21), we have the solution for all nine equations are

$$\theta_1 = \pm \arccos\left(\frac{\cos\alpha}{1-\cos\alpha}\right), \tag{27a}$$

or

$$\theta_1 = \pm \arccos\left(\frac{-2-\cos\alpha}{1-\cos\alpha}\right), \tag{27b}$$

and

$$\theta_2 = -\theta_1, \quad \theta_3 = \theta_1. \tag{28}$$

Considering (26) and (28), we have

$$\theta_1 = \theta_3 = \theta_5, \tag{29a}$$

$$\theta_2 = \theta_4 = \theta_6 = -\theta_1. \tag{29b}$$

So (27) and (29) are the closure equations for the six-link close-loop with the geometric condition (7). In fact, there are six independent equations in (27) and (29). When the twist α is given, there are two or four fixed solutions for the kinematic variables, $\theta_i (i = 1, 2, \ldots, 6)$. Therefore the close-loop is not a linkage but a structure. In the compatibility space, it is presented by the individual point as shown in Fig. 6a.

There are also a number of characteristics of the structural closure, which can be found from the six equations (27) and (29).

1. When $-\frac{\pi}{3} < \alpha < \frac{\pi}{3}$, there is no structural closure;
2. when $\alpha = \pm\frac{\pi}{3}$, $\theta_i = 0$ $(i = 1, 2, \ldots, 6)$. This planar close-loop is a structure, which has infinitesimal mobility;
3. when $-\frac{2\pi}{3} < \alpha < -\frac{\pi}{3}$ and $\frac{\pi}{3} < \alpha < \frac{2\pi}{3}$, only (27a) has two solutions. So there are only two structural closures. One example is shown in Fig. 6(b) for $\alpha = \arccos(1/3)$. They are in the same configuration, see Fig. 7;

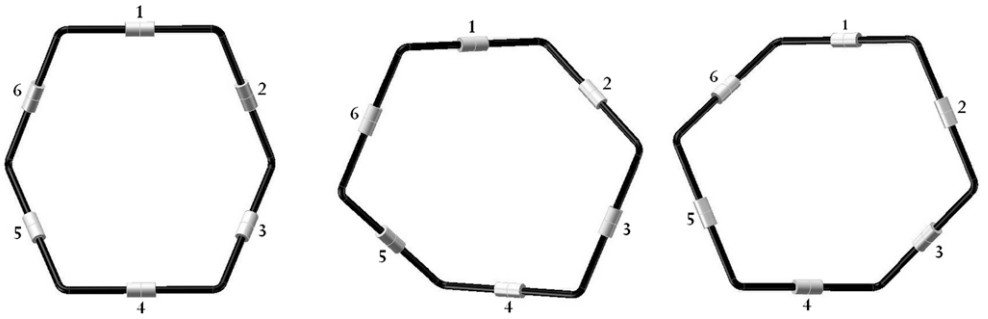

Fig. 4. The motion sequence of model with $\alpha = \arccos(1/3)$.

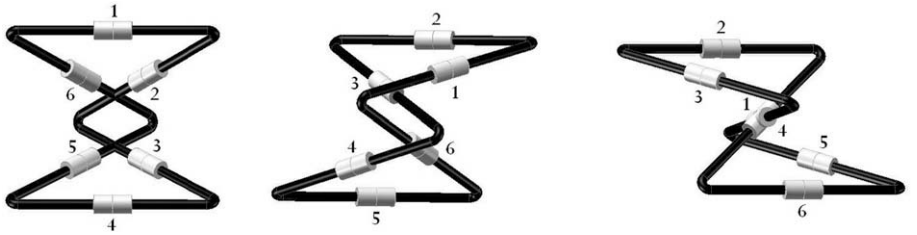

Fig. 5. The motion sequence of model with $\alpha = \frac{3\pi}{4}$.

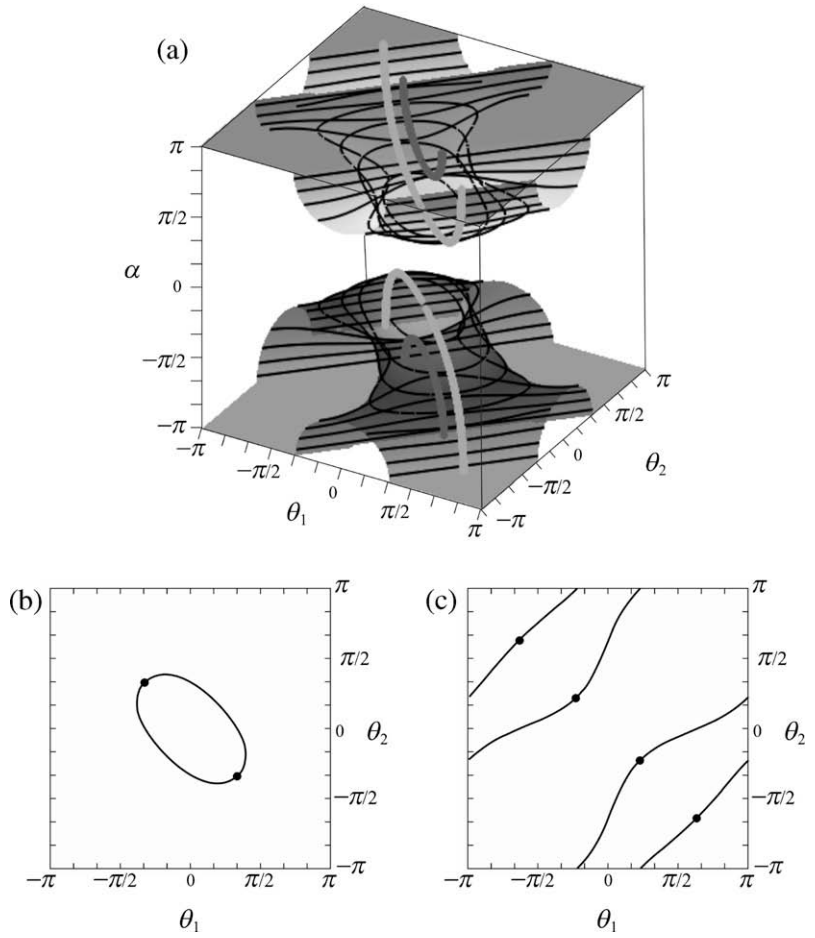

Fig. 6. The kinematic path of θ_2 vs. θ_1 for different twist α for both linkage and structure. (a) in 3D (surface is the kinematic paths and thick lines are the position of structural closure); (b) for $\alpha = \arccos(1/3)$; (c) for $\alpha = \frac{3}{4}\pi$. (In (b) and (c), curves are the kinematic paths, and point is the positions of structural closure.)

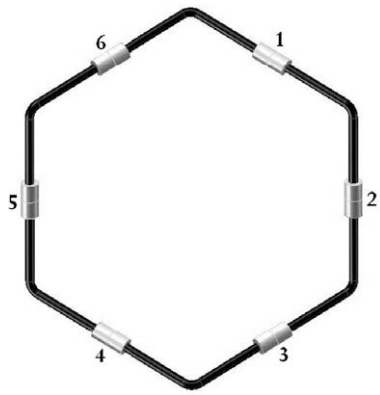

Fig. 7. The structural closure of $\alpha = \arccos(1/3)$.

4. when $-\pi \leqslant \alpha \leqslant -\frac{2\pi}{3}$ and $\frac{2\pi}{3} \leqslant \alpha \leqslant \pi$, both (27a) and (27b) have two solutions. So there are four structural closures. One example is shown in Fig. 6c for $\alpha = \frac{3}{4}\pi$. Every two of them in the same configuration, see Fig. 8;
5. linkages with twist α and $-\alpha$ have the same structural closures due to the different setup of geometric parameters; and
6. (29) shows that the structural closures have threefold rotational symmetry and three symmetry planes. So it is threefold-symmetric.

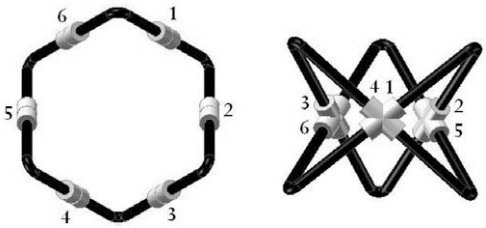

Fig. 8. The two structural closures of $\alpha = \frac{3}{4}\pi$.

4. Conclusions and discussion

In this paper, the closure equation of the assembly of six identical links with zero length and same twist connected by six identical revolute joints with same offset has been analysed with matrix method. Two closure forms have been found. One is the special mobile line-symmetric octahedral case of Bricard linkage, while the other is a structure in one or two kinds of closed loops. Both closure forms have been identified on the compatibility space by curves and points, respectively.

Stationary configurations of the linkage form have also been analysed. They are the configurations when any joint angle of the linkage is in its maximum or minimum. When θ_1 is at its maximum or minimum, we have

$$\frac{d\theta_1}{d\theta_2} = 0, \tag{30a}$$

and

$$\frac{d\theta_1}{d\theta_3} = 0. \tag{30b}$$

Differentiating the closure equations (23)–(25), we can get that for $\alpha \in \left[\frac{\pi}{3}, \frac{2\pi}{3}\right]$, the stationary configuration is at

$$C\theta_1 = \frac{1}{2}\left(\frac{1+2C\alpha}{1-C\alpha} - \frac{\sqrt{3}}{S\alpha}\right) \quad \text{and} \quad C\theta_2 = C\theta_3 = \frac{\sqrt{3}}{S\alpha} - 1. \tag{31a}$$

And for $\alpha \in \left[-\frac{2\pi}{3}, -\frac{\pi}{3}\right]$, the stationary configuration is at

$$C\theta_1 = \frac{1}{2}\left(\frac{1+2C\alpha}{1-C\alpha} + \frac{\sqrt{3}}{S\alpha}\right) \quad \text{and} \quad C\theta_2 = C\theta_3 = -\frac{\sqrt{3}}{S\alpha} - 1, \tag{31b}$$

which is the same result given in [5].

In order to apply this special closed assembly into the field of reconfigurable mechanism, the transformation between the special Bricard octahedral linkage and the structure closure shall be studied next. Currently, the two forms can only be transferred by opening the close-loop and reassembling after changing the kinematics variables. An automatic approach shall be explored for feasible engineering applications.

References

[1] R. Bricard, Mémoire sur la théorie de l'octaedre articulé. Journal de mathématiques pures et appliquées, Liouville 3 (1897) 113–148.
[2] R. Bricard, Leçons de cinématique, Tome II Cinématique Appliquée, Gauthier-Villars, Paris, 1927. p. 7–12.
[3] J.E. Baker, An analysis of Bricard linkages, Mechanism and Machine Theory 15 (1980) 267–286.
[4] G.T. Bennett, Deformable octahedra, Proceeding of London Mathematics Society, 2nd series 10(1) (1911) 309–343.
[5] J.E. Baker, Limiting positions of a Bricard linkage and their possible relevance to the cyclohexane molecule, Mechanism and Machine Theory 21 (3) (1986) 253–260.
[6] J.E. Baker, A compendium of line-symmetric four-bars, Transactions of the ASME: Journal of Mechanical Design 101 (1979) 509–514.
[7] J. Phillips, Freedom of Machinery, Vol. II, Cambridge University Press, Cambridge, 1990.
[8] J. Denavit, R.S. Hartenberg, A kinematic notation for lower-pair mechanisms based on matrices, Journal of Applied Mechanics 22 (2) (1955) 215–221.
[9] Y. Chen, Z. You, Two-fold symmetrical 6*R* foldable frames and their bifurcations, International Journal of Solids and Structures 46 (25–26) (2009) 4504–4514.